THIS DOCUMENT IS DEPRECATED. PLEASE REFER TO:

https://gitlab.com/openpolarradar/opr/-/wikis/Radar-Guide

Radar Depth Sounder

Summary

To better understand processes affecting the ice sheets and to supply boundary condition information into ice sheet models and ice thickness for other ice sheet analysis, the Center for Remote Sensing of Ice Sheets (CReSIS) and formerly the Radar Systems and Remote Sensing Laboratory (RSL) have designed, developed, and deployed radar depth sounders since 1987 (Raju, Xin, and Moore 1990). While this dataset contains data from many radar system versions spanning 1993 to the present, the general purpose of the measurements and the output data product format is largely unchanged.

The RDS data set contains Geolocated Radar Echo Strength Profile Images (L1B data), Ice Thickness, Ice Surface, and Ice Bottom elevations (L2 data), and Gridded Ice Thickness, Ice Surface, and Ice Bottom elevations (L3 data) over Greenland, Canada, and Antarctica taken with the CReSIS Radar Depth Sounders.

The L1B dataset includes geocoded radar images known as echograms. The data files contain the echograms, UTC time, latitude, longitude, elevation, and aircraft attitude. The data files are provided in Mathworks Matlab file format. The data files are also provided in pdf and jpg formats for each of browsing.

The L2 dataset includes measurements for UTC time, latitude, longitude, elevation, surface, bottom, and thickness. The data files are provided in CSV format.

The L3 data set includes grids of L2 data for time, latitude, longitude, elevation, surface, bottom, and thickness. This data set is a merging of several data sources: radar depth sounder over multiple seasons, airborne LIDAR data for the ice surface, optical data for ice boundaries, and various ice surface digital elevation models for the ice surface to fill in where no LIDAR is available.

The radar depth sounder data have been collected on an ongoing basis since 1993 using grant funding from NASA and NSF. The most recent data were collected as part of the NSF Science and Technology Center grant (ANT-0424589) and the NASA Operation IceBridge field campaign (NNX16AH54G).

The data are stored in MATrix LABoratory (MATLAB) files with associated PDF, CSV, and PNG files.

The data are available at ftp://data.cresis.ku.edu/ and https://data.cresis.ku.edu/. These two sites serve the same data, but use the ftp (port 21) and https (port 443) protocols respectively.

Raju, G., W. Xin and R. K. Moore. 1990. Design, development, field observations, and preliminary results of the coherent Antarctic radar depth sounder (CARDS) of the University of Kansas, U.S.A.] Glacial., 36(123), 247- 254.

FAQ

The most convenient way to browse the imagery quickly is through the PDF files in the pdf directory.

The quickest way to plot the whole L2 dataset is to look at the browse files (KML or CSV) for the whole season in one of the two csv or kml directories depending on whether you want the whole flight line (csv or kml) or just flight lines with good ice bottom data (csv_good or kml_good).

The standard L1B files are, in order of increasing quality, CSARP_qlook, CSARP_csarp-combined, CSARP_standard, and CSARP_mvdr directories. These are located in ftp://data.cresis.ku.edu/data/rds/{$season_name}/. Each directory will contain a complete set of echograms so downloading a single directory (usually the highest quality available) is what we recommend.

The standard L2 files are in the ftp://data.cresis.ku.edu/data/rds/{$season_name}/csv directory. A variety of options are available so that you can download the data in a single file or in smaller chunks if you know what you are looking for. We also have two geographic search utilities at ftp://data.cresis.ku.edu/data/geographic_search/ that let you select data geographically. The utility finds all the data segments and frames from the region of interest and optionally downloads the L2 data for you.

The L3 files are in the ftp://data.cresis.ku.edu/data/grids/ directory.

For the highest quality and most complete browsing of the data, use the Matlab image browser at ftp://data.cresis.ku.edu/data/picker/. The guide for the picker also explains the surface and bottom layer tracking process.

Mathworks MAT file readers for C and IDL including documentation from Mathworks are located at ftp://data.cresis.ku.edu/data/mat_reader/.

Data Organization

The radar data are divided into segments. A segment is a contiguous dataset where the radar settings do not change. A day is divided into segments if the radar settings were changed, hard drives were switched, or other operational constraints required that the radar recording be turned off and on. The segment ID is YYYYMMDD_SS where YYYY is the 4-digit year (e.g. 2011), MM is the 2-digit month from 1 to 12, DD is the 2-digit day of the month from 1 to 31, and SS is the segment number from 0 to 99. Segments are always sorted in the order in which the data was collected. Generally SS starts with 1 and increments by 1 for each new segment, but this is not always the case: only the ordering is guaranteed to match the order of data collection.

Each segment is broken into frames (analogous to satellite SAR scenes) to make analyzing the data easier. Most frames are 50-km long, but some of them may be longer or shorter so that the breaks between frames lie at convenient locations. For example, if a grid is flown, we try to align the frames from adjacent lines. Once the frame boundaries are defined, they will not change from one release to the next or one processing method to the next. The frame ID is a concatenation of the segment ID and a frame number and follows the format YYYYMMDD_SS_FFF where FFF is the frame number from 000 to 999. Frames may overlap slightly so that data are duplicated where the overlap occurs. Generally the FFF starts with 0 or 1 and increments by 1 for each new frame, but this is not always the case: only the ordering is guaranteed to match the order of data collection.

In a data casting sense, the data granule for L1B and L2 data is the frame.

File Descriptions

On the ftp://data.cresis.ku.edu/data/rds/ page, L1B and L2 files are in the radar depth sounder folder (rds), arranged by Season ID (e.g. 2011_Greenland_P3) and L3 files are available at ftp://data.cresis.ku.edu/data/grids. Since L1B and L2 files are specific to a season and contain only radar depth sounder data, these files are stored together in the season ID folders under the directory rds. The L3 files contain data from multiple sources and seasons and are stored under a separate folder because of this.

L1B products

CSARP_{$processing_type}/{$segment_id}/Data{$image_id}_{$frame_id}.mat

For each data frame there may be many different L1B products depending on how waveforms, and channels are combined and how the processing is done. More details about the standard outputs are given in the Methods section. A few example filenames are:

CSARP_qlook/20110516_01/Data_img_01_20110516_01_006.mat
CSARP_csarp-combined/20110516_01/Data_20110516_01_006.mat

The {$processing_type} is a string. The common processing types are qlook, csarp-combined, standard, and mvdr.

The {$segment_id} is explained in the Data Organization section.

The {$image_id} is a string which may be empty when it is a composite image or is of the form “img_II” where II is the 2-digit zero-padded image number always starting with 1 and incrementing from there. Images are explained in the Derivation Techniques and Methods.

The {$frame_id} is explained in the Data Organization section.

The file format is Matlab .MAT version 6.

images/{$segment_id}/{$frame_id}_HHmmss_{0maps,1echo,2echo_picks}.jpg

For each data frame there is a flight path file (0map), an echogram file (1echo), and an echogram overlaid with surface and bottom picks (2echo_picks). The background images are Landsat-7 natural color imagery in polar stereographic format (70 deg true scale latitude, -45 deg longitude is center for Greenland/Canada and -71 deg true scale latitude, 0 deg longitude is center for Antarctica). A few example filenames are:

images/20110507_01/20110507_01_001_110941_0maps.jpg
images/20110507_01/20110507_01_001_110941_1echo.jpg
images/20110507_01/20110507_01_001_110941_2echo_picks.jpg

HHmmss is the GPS time stamp for the first range line in the image where HH is 00-23 hours, mm is 00-59 minutes, and ss is 00-59 seconds.

The echogram images are generated from the csarp-combined data product or the standard data product.

The file format is JPEG.

L2 products

csv/{$segment_id}/Data_{$frame_id}_HHmmss.csv

Contains the ice surface and ice bottom layer information. There is one file per data frame. An example filename is:

csv/20110407_06/Data_20110407_06_001_151055.csv

HHmmss is the GPS time stamp for the first range line in the csv file where HH is 00-23 hours, mm is 00-59 minutes, and ss is 00-59 seconds.

The file format is comma separated variable (CSV).

csv/Data_{$segment_id}.csv

These files are provided for ease of download and file transfer. They are the same format as the individual data frame CSV files. These files have all the individual frames from the segment concatenated together. An example filename is

csv/Data_20110331_09.csv

csv/{$season_id}.csv

These files are provided for ease of download and file transfer. They are the same format as the individual data frame CSV files. These files have all the individual frames from the whole season concatenated together.

The {$season_id} is a string that is formatted as YYYY_location_platform, YYYY is the 4-digit year *of when the season began*, location is the geographic location (e.g. Greenland or Antarctica), and platform is the airborne system used (e.g. P3, TO, DC8, Ground).

An example filename is:

csv/2011_Greenland_P3.csv

csv/Browse_{$season_id}.csv

The save as the whole season CSV file except only every 50th point is taken to keep the file size small.

csv/Browse_2011_Greenland_P3.csv

csv_good/

All the same files as csv except files only contain data points where the ice surface and ice bottom were detected.

layerData/{$segment_id}/Data_{$frame_id}.mat

For each data frame there is a layer data file. This file contains the full layer information for the ice surface, ice bottom and any other layers that have been picked *and is required by the image browser/layer picker*. An example filename is:

CSARP_layerData/20110516_01/Data_20110516_01_006.mat

The file format is Matlab .MAT version 6.

Browsing Files

pdf/{$segment_id}.pdf

Same images as the files in the images directory, except all images from a segment are concatenated into a single PDF file for convenient browsing and file transfer.

kml/

Browse_Data_{$segment_id}.kml

Browse_{$season_id}.kml

These files are for geographically browsing the files. Only a few data points are included to allow for quick download and browsing. We produce one KML file per segment and then one KML with all segments (entire season). The per segment files contain information per frame and more data points. The season file contains information for each segment and fewer data points.

kml_good/

All the same files as kml except files only contain data points where the ice surface and ice bottom were detected.

{$radar_id}_param_{$season_id}.xls

This spreadsheet file allows all of the radar and processing parameters to be browsed conveniently. These parameters are encapsulated in the L1B data files, but this spreadsheet provides another way to access this information. An example filename is:

mcords2_param_2011_Greenland_P3.xls

The {$radar_id} is a string containing the radar ID which is one of icards, acords, mcrds, mcords, or mcords2.

General utilities and documents

ftp://data.cresis.ku.edu/data/gps_ins/

See guide in this folder for more details. The individual GPS/INS files are stored with this naming convention:

{$season_id}/gps_YYYYMMDD.mat

A few examples are:

2011_Greenland_P3/gps_20110507.mat
2011_Greenland_P3/gps_20110516.mat

The file format is Matlab .MAT version 6.

ftp://data.cresis.ku.edu/data/mat_reader/

Matlab MAT file reader for Matlab, C, and IDL. See guide in this folder for more details.

ftp://data.cresis.ku.edu/data/picker/

Echogram browsing tool (currently requires Matlab). See guide in this folder for more details

ftp://data.cresis.ku.edu/data/geographic_search/

Basic geographic search tool (currently requires Matlab). Convenient for searching all of the seasons of data and listing all of the frames and segments of interest.

ftp://data.cresis.ku.edu/data/segy/

SEGY and SEG2 converter information – currently not available. We have used SEGYMAT, but do not have any support functions available. Below are some links to SEGYMAT and the SEGY and SEG2 formats.

http://segymat.sourceforge.net/
http://www.seg.org/documents/10161/77915/seg_2.pdf
http://www.seg.org/documents/10161/77915/seg_y_rev1.pdf
http://www.seg.org/documents/51956/6062543/SEGY+Rev+2+Draft+March+2014

ftp://data.cresis.ku.edu/data/rds/rds_readme.doc

The most recent version of this readme file.

L1B Matlab Files

When one-image is used alone, there is just one file for each type of processing. For example:

- Data_img_01_20100106_01_001.mat

When two-images are created, the two images are combined into a single image. The first image is formed from data with low-gain settings for the air/ice interface and upper-ice layers retrieval, and the second image is formed from data with high-gain settings for the ice/bottom interface and deep-ice layer retrieval. They are combined at a fixed time after the surface return. The fixed time is approximately the same as the high-gain setting pulse duration. The individual waveforms are also stored. For example:

- Data_20091224_01_001.mat (combined)
- Data_img_01_20091224_01_001.mat (individual)
- Data_img_02_20091224_01_001.mat (individual)

For files at NSIDC, there is just one echogram file per data frame and it always has a name of this format even when only one-image is used (i.e. the “img_01” is removed):

- Data_20100106_01_001.mat

CSARP_qlook

This L1B product uses unfocused synthetic aperture radar processing. This means that the data are coherently stacked (i.e. each set of N range lines is averaged in slow time with no correction for propagation delay changes). The data are not motion compensated. The array processing simply adds the channels together.

CSARP_csarp-combined

This L1B product uses focused synthetic aperture radar processing, but does not apply motion compensation. Also, the channels are added together before SAR processing.

CSARP_standard

This L1B product uses focused synthetic aperture radar processing on each channel separately. Motion compensation is applied. We apply periodogram direction of arrival estimation (i.e. delay-and-sum beam forming) to combine the channels during array processing. Different windows may be applied to form the periodogram (usually boxcar or hanning).

CSARP_mvdr

This L1B product is the same as standard except the array processing uses the minimum variance distortionless reponse (MVDR) beam former. This is a data dependent technique that forms a data covariance matrix using SAR subapertures or neighboring pixels to estimate and remove the noise. While it tends to have better clutter rejection compared to the periodogram, it also suffers from a self-nulling problem. This self-nulling means that the desired signal is sometimes mistaken for the “noise” and MVDR actually suppresses the signal. This tends to happen when the signal is strong relative to the noise. Because of this, MVDR should not be used in applications that require any kind of radiometric fidelity.

CSARP_music

This L1B product is the same as standard except the array processing uses the multiple signal classification (MUSIC) beam former. This is a data dependent technique that forms a data covariance matrix using SAR subapertures or neighboring pixels to estimate and remove the noise. While it tends to have better clutter rejection compared to the periodogram, it also tends to not do as well is very low signal to noise ratio situations and when the array (steering vectors) or scene (number of signals) do not fit the model well.

Mat File Description

Each Matlab (.mat) file has the following variables:

Name	Data
Size/Axes	M by N double array where M is fast time and N is slow time
Units	Relative received power (Watts)
Range	Full double range
Null Value	NA
Description	Radar echogram data

Name	Time
Size/Axes	M by 1 double vector where M is fast time
Units	Seconds
Range	Full double range
Null Value	NA
Description	Fast time (zero time is the beginning of the transmit event calibrated to within one range resolution cell). This is two-way travel time or propagation delay for each range bin in Data.)

Name	Depth
Size/Axes	M by 1 double vector where M is fast time
Units	Meters
Range	Full double range
Null Value	NA
Description	Range axis assuming a vacuum media (Depth = Time * c/2)

Name	GPS_time
Size/Axes	1 by N double vector where N is slow time
Units	Seconds
Range	Full double range
Null Value	NA
Description	GPS time when data were collected (seconds since Jan 1, 1970 00:00:00). This is the ANSI C standard.

Name	Latitude
Size/Axes	1 by N double vector where N is slow time
Units	Degrees
Range	-90 to +90
Null Value	Not a Number (indicates that no GPS information is available)
Description	WGS-84 geodetic latitude coordinate. Always referenced to North. Without motion compensation, represents the location that the trajectory data was processed to. With motion compensation, represents the location of the radar echogram data phase center. It may not be the actual measurement location due to motion compensation

Name	Longitude
Size/Axes	1 by N double vector where N is slow time
Units	Degrees
Range	-180 to +180
Null Value	Not a Number (indicates that no GPS information is available)
Description	WGS-84 geodetic longitude coordinate. Always referenced to East. Without motion compensation, represents the location that the trajectory data was processed to. With motion compensation, represents the location of the radar echogram data phase center. It may not be the actual measurement location due to motion compensation

Name	Elevation
Size/Axes	1 by N double vector where N is slow time
Units	Meters
Range	Full double range
Null Value	Not a Number (indicates that no GPS information is available)
Description	Referenced to WGS-84 ellipsoid. Positive is outward from the center of the Earth. Without motion compensation, represents the location that the trajectory data was processed to. With motion compensation, represents the location of the radar echogram data phase center. It may not be the actual measurement location due to motion compensation

Name	Surface
Size/Axes	1 by N double vector where N is slow time
Units	Seconds
Range	Full double range
Null Value	Not a Number (indicates that no surface information is available)
Description	Estimated two way propagation time to the ice surface from the phase center. This uses the same frame of reference as the Time variable. This information is used during SAR processing to determine where the dielectric half-space between air and ice should be – this is not the L2 product although they are often the same.

Name	Bottom
Size/Axes	1 by N double vector where N is slow time
Units	Seconds
Range	Full double range
Null Value	Not a Number (indicates that no bottom information is available)
Description	Estimated two way propagation time to the ice bottom from the phase center. This uses the same frame of reference as the Time variable. This information is used during 3D-imaging to determine where the ice bed may be – this is not the L2 product although they are often the same.

Name	*param* (multiple variables with a name containing the string "param")
Size/Axes	NA, data structures
Units	NA
Range	NA
Null Value	NA
Description	Contains: 1) Radar and processing settings, 2) Processing software version and time stamp information. Fields of structures are not static and may change from one version to the next. Fields are only available when the data has been processed through the new processing pipeline.

NetCDF File Description

Each NetCDF (.nc) file has the following variables:

L2 Matlab Files

Name	GPS_time
Size/Axes	1 by N double vector where N is slow time
Units	Seconds
Range	Full double range
Null Value	NA
Description	GPS time when data were collected (seconds since Jan 1, 1970 00:00:00). This is the ANSI C standard.

Name	Latitude
Size/Axes	1 by N double vector where N is slow time
Units	Degrees
Range	-90 to +90
Null Value	Not a Number (indicates that no GPS information is available)
Description	WGS-84 geodetic latitude coordinate. Always referenced to North. Without motion compensation, represents the location that the trajectory data was processed to. With motion compensation, represents the location of the radar echogram data phase center. It may not be the actual measurement location due to motion compensation.

Name	Longitude
Size/Axes	1 by N double vector where N is slow time
Units	Degrees
Range	-180 to +180
Null Value	Not a Number (indicates that no GPS information is available)
Description	WGS-84 geodetic longitude coordinate. Always referenced to East. Without motion compensation, represents the location that the trajectory data was processed to. With motion compensation, represents the location of the radar echogram data phase center. It may not be the actual measurement location due to motion compensation.

Name	Elevation
Size/Axes	1 by N double vector where N is slow time
Units	Meters
Range	Full double range
Null Value	Not a Number (indicates that no GPS information is available)
Description	Referenced to WGS-84 ellipsoid. Positive is outward from the center of the Earth. Without motion compensation, represents the location that the trajectory data was processed to. With motion compensation, represents the location of the radar echogram data phase center. It may not be the actual measurement location due to motion compensation.

Name	layerData{layer_idx}
Size/Axes	1 x P cell array of structures, where P is the number of layers
Units	NA
Range	NA
Null Value	NA
Description	The first layer (layer_idx = 1) is the ice surface. For the depth sounder, the second layer (layer_idx = 2) is the ice bottom.

Name	layerData{layer_idx}.name
Size/Axes	character array, arbitrary length
Units	NA
Range	NA
Null Value	NA
Description	Name of the layer ("surface" and "bottom" are reserved for ice surface and ice bottom respectively)

Name	layerData{layer_idx}.value{pick_idx}
Size/Axes	1 by 2 cell array of structures
Units	NA
Range	NA
Null Value	NA
Description	There are two pick types: the manual picks are stored in pick_idx = 1 and the automated picks are stored in pick_idx = 2.

Name	*layerData{ layer_idx}.value{pick_idx}.data*
Size/Axes	1 by N double vector
Units	Seconds
Range	Full double range
Null Value	Not a Number (indicates that no surface information is available for this particular index and pick type)
Description	Estimated two way propagation time to the layer from the collection platform.

Name	*layerData{ layer_idx}.quality*
Size/Axes	1 by N double vector
Units	NA
Range	1, 2, or 3 (a value of NaN or 0 means the quality has not been assigned)
Null Value	NA
Description	Quality level of the data (1-3), 1 represents high confidence, 2 represents low confidence or large error bars, and 3 represents a derived or estimated result based on information beyond just the present data frame

CSV Files

Each comma-separated variable (CSV) file has the following fields in the order given below. The first four fields are the standard fields that CReSIS has used for a number of years in its data products. Five new fields have been added in this data product.

- Latitude (deg North)
- Longitude (deg East)
- UTC Time (seconds of day)
    - Full time information is provided by looking at the Frame ID field
- Thickness (meters)
    - This is Bottom minus Surface
    - Constant dielectric of 3.15 (no firn) is assumed for converting propagation delay into range.
    - -9999 indicates no thickness available
- Elevation (meters)
    - Referenced to WGS-84 Ellipsoid
- Frame ID (YYYYMMDDSSFFF)
    - Fixed length numeric field where YYYY = year, MM = month, DD = day, SS = segment, FFF = frame
- Surface (meters)
    - Range to ice surface. The actual surface height is Elevation minus this number
- Bottom (meters)
    - Range to ice bottom. The actual ice bottom height is Elevation minus this number
    - Constant dielectric of 3.15 (no firn) is assumed for converting propagation delay into range.
    - -9999 indicates no thickness available
- Quality level
    - 1: High confidence pick
    - 2: Medium confidence pick
    - 3: Low confidence pick

Here is an example of the headers and a single row of data. The precision is fixed.

LAT	LON	UTCTIMESOD	THICK	ELEVATION
-76.981716	-99.865364	4959.6484	2347.47	1877.2312

FRAME	SURFACE	BOTTOM	QUALITY
2010010502005	570.13	2917.59	1

Theory of Measurements:

A variety of instruments have been used to produce these data products. The concept rests on the fact that when a pulse of RF energy is transmitted into the ice sheet, a portion of the energy is reflected from the ice surface, ice bottom, and any englacial targets – generally anywhere there is a contrast in the (electromagnetic) constitutive properties of the media. Since we are interested in detecting the ice bottom, lower frequencies are used because they do not attenuate as quickly through ice (Paden 2005).

Radar Systems

The following table lists the different radar systems that have been used since 1993 with references and basic system properties. The original introduction of each radar system is bolded. Modifications were often made to each radar system and only the deviations from the previous installation of the radar system on a particular platform (e.g. “MCoRDS 2 on P3”) are noted. The performance of the radar system is dependent on platform because the antenna installation varies between platforms and may affect the number of transmit and receive channels and the frequency range.

SeasonID	Reference	Description
1993 Greenland P3	Chuah 1997 Gogineni 1998;	**Improved Coherent radar depth sounder (ICORDS)** Bandwidth: 141.5-158.5 MHz Tx power: 200 W Pulse duration: 1.6 us Waveform: Analog chirp generation (SAW) Acquisition: Single channel 8 bit ADC, 18.75 MHZ IQ sampling (coherent averaging, but incoherent recording only) Dynamic Range: Sensitivity timing control Rx aperture: 2 wavelengths (4 dipoles) Tx aperture: 2 wavelengths (4 dipoles) Bistatic Rx/Tx Data rate: ~0.05 MB/sec
1995 Greenland P3		ICORDS
1996 Greenland P3		ICORDS
1997 Greenland P3		ICORDS Some data segments collected in coherent mode.
1998 Greenland P3	Akins 1999; Gogineni 2001	**ICORDS 2 (ICORDS2)** Bandwidth: 141.5-158.5 MHz Tx power: 200 W Pulse duration: 1.6 us Waveform: Analog chirp generation (SAW) Acquisition: Single channel 12 bit ADC, 18.75 MHz IQ sampling Dynamic Range: Sensitivity timing control Rx aperture: 2 wavelengths (4 dipoles) Tx aperture: 2 wavelengths (4 dipoles) Bistatic Rx/Tx Data rate: ~0.5 MB/sec
1999 Greenland P3		ICORDS2
2001 Greenland P3		ICORDS2
2002 Greenland P3		ICORDS2
2002 Antarctica P3chile		ICORDS2 on Chilean Navy P-3
2003 Greenland P3	Namburi 2003	**Advanced Coherent Radar Depth Sounder (ACORDS)** Bandwidth: 140-160 MHz Tx power: 200 W Waveform: Single channel chirp generation Acquisition: Single channel Dynamic Range: low and high gain channels Rx aperture: 2 wavelengths (4 dipoles) Tx aperture: 2 wavelengths (4 dipoles) Bistatic Rx/Tx Data rate: 20 MB/sec

2004 Greenland Ground	Kuchikulla 2004	**Wideband Coherent Radar Depth Sounder (WCRDS)** Bandwidth: 50-200 MHz Tx power: 200 W Waveform: Single channel chirp generation Acquisition: Single channel Dynamic Range: low and high gain channels Rx aperture: 2 wavelengths (4 TEM horns) Tx aperture: 2 wavelengths (4 TEM horns) Bistatic Rx/Tx Data rate: 20 MB/sec
2004 Antarctica P3chile		ACORDS on Chilean Navy P-3 Acquisition: Single channel or five channels multiplexed to a single channel depending on data segment.
2005 Greenland TO		ACORDS on Twin Otter Acquisition: Single channel or five channels multiplexed to a single channel depending on data segment. Rx aperture: 2.5 wavelengths (5 folded dipoles) Tx aperture: 2.5 wavelengths (5 folded dipoles)
2005 Greenland Ground	Paden 2006; Paden 2010	**Synthetic Aperture Radar (SAR)** Bandwidth: 120-300 MHz Tx power: 800 W Waveform: Single channel chirp generation Acquisition: Eight channels (multiplexed to two simultaneous), 8 bit ADC at 720 MHz bandpass sampling Dynamic Range: waveform playlist Rx Aperture: 4 wavelength (8 TEM horns) Tx Aperture: 0.5 wavelength; ping-pong with 3.5 wavelength baseline (2 TEM horns per side) Bistatic Rx/Tx Data rate: 30 MB/sec total
2005 Antarctica Ground		SAR Bandwidth: 120-300 MHz (low SNR restricted to 140-160 MHz)
2006 Greenland TO	Lohoefener 2006	**Multi-Channel Radar Depth Sounder (MCRDS)** Bandwidth: 140-160 MHz Tx power: 800 W (two 400 W amps are power split to 5 antennas) Waveform: Single channel chirp generation Acquisition: Eight channels, 12 bit ADC at 125 MHz bandpass sampling Dynamic Range: waveform playlist Rx Aperture: 3 wavelength aperture (5 dipoles) Tx Aperture: 3 wavelength aperture; but configurable for ping-pong operation (5 dipoles) Bistatic Rx/Tx Data rate: 30 MB/sec total

2007 Greenland P3		MCRDS on P3 Tx power: 800 W (two 400 W amps are power split to 4 antennas) Bandwidth Selection: 140-160 MHz or 435-465 MHz Rx Aperture: 2 wavelength aperture (4 dipoles) Tx Aperture: 2 wavelength aperture (4 dipoles)
2008 Greenland TO		MCRDS on TO Tx power: 800 W (two 400 W amps are power split to 6 antennas) Rx Aperture: 3 wavelength aperture (6 dipoles) Tx Aperture: 3 wavelength aperture; but configurable for ping-pong operation (6 dipoles)
2008 Greenland Ground		MCRDS at NEEM Bandwidth: 135-165 MHz Tx power: 400 W Rx Aperture: 4 wavelength aperture (8 log-periodic) Tx Aperture: 0.5 wavelength aperture; ping-pong with 3.5 wavelength baseline (1 log-periodic) Polarimetric
2008 Greenland Gambit		MCRDS on Gambit Tx power: ? W Rx Aperture: 2 wavelength aperture (4 dipoles) Tx Aperture: 2 wavelength aperture (4 dipoles)
2008 Antarctica Ground		MCRDS at WAIS ?
2008 Antarctica Gambit		MCRDS on Gambit
2009 Greenland TO		MCRDS on TO
2009 Antarctica DC8	Ledford 2009; Rodriguez-Morales 2010; Player 2010; Li 2011; Allen 2011	**Multi-Channel Coherent Radar Depth Sounder (MCoRDS)** Bandwidth: 180-210 MHz (DC-8 platform restricted to 189.15-198.65 MHz) Tx power: 500 W (100W/channel) Waveform: Eight channel chirp generation Acquisition: Eight channels, 14 bit ADC at 111 MHz bandpass sampling Dynamic Range: waveform playlist Rx Aperture: 1.5 wavelength aperture Tx Aperture: 1.5 wavelength aperture; fully programmable Monostatic Rx/Tx Data rate: 12 MB/sec per channel
2009 Antarctica TO		MCoRDS on TO (v1) Bandwidth: 140-160 MHz Tx power: 600 W (100W/channel) Rx Aperture: 3 wavelength aperture Tx Aperture: 3 wavelength aperture; fully programmable Bistatic Rx/Tx
2010 Greenland DC8		MCoRDS on DC8

2010 Greenland P3	Byers 2011	MCoRDS on P3 Bandwidth: 180-210 MHz (EMI restricted to 10 MHz within 180-210 MHz most segments) Tx power: 700 W (100 W/channel) Acquisition: Sixteen channels (multiplexed on to 8 channels), 14 bit ADC at 111 MHz bandpass sampling Rx Aperture: 2 wavelength, 3.5 wavelength, and 2 wavelength apertures, baseline of 6.4 m between each aperture Tx Aperture: 3.5 wavelength aperture; fully programmable Mixed monostatic and bistatic tx/rx Data rate: 6 MB/sec per channel
2010 Antarctica DC8		MCoRDS on DC8 Tx power: 500 W (100 W/channel) Dynamic Range: waveform playlist coupled with low gain and high gain channels
2011 Greenland TO		MCoRDS on TO (v2) Tx power: 600 W (100 W/channel) Acquisition: Sixteen channels (multiplexed on to 8 channels), 14 bit ADC at 111 MHz bandpass sampling Rx Aperture: Two 3 wavelength apertures with 13.8 m baseline Tx Aperture: 3 wavelength aperture; fully programmable Mixed monostatic and bistatic tx/rx Data rate: 6 MB/sec per channel
2011 Greenland P3	Rodriguez 2014	**MCoRDS 2 on P3** Bandwidth: 180-210 MHz Tx power: 1050 W (150W/channel, used only 75 W/channel or 525W total due to antenna limitations) Waveform: Eight channel chirp generation Acquisition: Sixteen channels (fifteen used), 14 bit ADC at 111 MHz bandpass sampling Dynamic Range: waveform playlist Rx Aperture: Left wing array: 2 wavelength and four channels, fuselage array: 3.5 wavelength and seven channels, right wing array: 2 wavelength and four channels, baseline of 6.4 m between each array Tx Aperture: 3.5 wavelength aperture; fully programmable Receive only on wing arrays and tx/rx on center array Data rate: 32 MB/sec per channel

2011 Antarctica DC8		MCoRDS on DC8 Tx power: 750 W (150W/channel) Notes: Waveform playlist coupled with low gain and high gain channels (3 channels were permanently low gain). This was done because of slow switching time of TR switch.
2011 Antarctica TO		MCoRDS 2 on TO Tx power: 1500 W (250W/channel) Rx Aperture: Two 3 wavelength apertures with 13.8 m baeseline Tx Aperture: 3 wavelength aperture; fully programmable Notes: Upgraded transmit-receive switch
2012 Greenland P3		MCoRDS 2 on P3 Notes: Tx power: 1050 W (150W/channel, 300W for center channel to account for poor nadir gain) Old transmit-receive switches
2012 Antarctica DC8		MCoRDS 2 on DC8 Tx power: 1250 W (250W/channel) Notes: Upgraded transmit-receive switch Five receive channels
2013 Greenland P3		**MCoRDS 3 on P3** Notes: For this season only, the wing arrays were not installed. Upgraded transmit-receive switch System identical to mcords2 except for a digital system file header change.
2013 Antarctica P3		MCoRDS 3 on P3
2013 Antarctica Basler	Wang 2015	**MCoRDS 4** on Polar6 Bandwidth: 150-450 MHz Tx power: 2000 W (250W per channel) Waveform: Eight channel chirp generation Acquisition: 8 channels, 12 bit ADC at 1600 MHz sampling Dynamic Range: waveform playlist Rx Aperture: 3.84 m array (2.5 wavelengths at 195 MHz) Tx Aperture: Same as Rx; each of 8 channels is fully programmable Monostatic tx/rx Data rate: 300 MB/sec aggregate for all channels

2014 Greenland P3		MCoRDS 3 on P3 Tx power: 2100 W (1050W due to power leveling elements and low center antenna nadir gain, amps are 150-450 MHz 300W/channel but only used 180-210 MHz, note P-3 baluns are limited to 250 W per channel except center channel that can handle 500 W). The end result is an effective transmit power of 150W per channel.
2014 Antarctica DC8		MCoRDS 3 on DC8 Bandwidth: 165-215 MHz Tx power: 6000 W (1000W/channel) Waveform: Six channel chirp generation Acquisition: Six channels, 14 bit ADC at 150 MHz bandpass sampling Notes: New antenna array installed with 3 cross track by 2 along track elements. New higher power amplifiers installed. Modification to digital system sampling frequency to handle new bandwidth.
2015 Greenland C130	Hale 2016	**MCoRDS 5** on C130 Bandwidth: 180-450 MHz (commonly used 180-230 MHz) Tx power: 2000 W Waveform: Two channel chirp generation Acquisition: 2 channels, 12 bit ADC at 1600 MHz sampling Dynamic Range: waveform playlist Rx Aperture: Two channels with 0.5 m aperture (quarter of a wavelength aperture) Tx Aperture: Same as rx; each channel is fully programmable Monostatic tx/rx Data rate: 200 MB/sec aggregate for all channels
2015 Greenland Polar6		MCoRDS 5 on Polar6 Bandwidth: 150-600 MHz Tx power: 6000 W Waveform: Eight channel chirp generation Acquisition: 24 channels, 12 bit ADC at 1600 MHz sampling Dynamic Range: waveform playlist Rx Aperture: Three 3.7 m arrays (2.5 wavelengths at 195 MHz), 8.1 m baseline between arrays, 8 channels per array Tx Aperture: Center array is also transmit; each of 8 channels is fully programmable Mixed monostatic and bistatic tx/rx Data rate: 750 MB/sec aggregate for all channels

2016 Greenland P3		MCoRDS 5 on NOAA P3 Bandwidth: 150-450 MHz (varied some) Tx power: 600 W Waveform: Two channel chirp generation Acquisition: 2 channels, 12 bit ADC at 1600 MHz sampling Dynamic Range: waveform playlist Rx Aperture: Two channels with 0.61 m aperture (half-wavelength aperture) Tx Aperture: Same as rx; each channel is fully programmable Monostatic tx/rx Data rate: 200 MB/sec aggregate for all channels
2016 Greenland Polar6		MCoRDS 5 on Polar6 Bandwidth: 150-600 MHz Tx power: 6000 W (four 1000W and four 500 W elements) Waveform: Eight channel chirp generation Acquisition: 24 channels, 12 bit ADC at 1600 MHz sampling Dynamic Range: waveform playlist Rx Aperture: Three 3.7 m arrays (2.5 wavelengths at 195 MHz), 8.1 m baseline between arrays, 8 channels per array Tx Aperture: Center array is also transmit; each of 8 channels is fully programmable Mixed monostatic and bistatic tx/rx Data rate: 750 MB/sec aggregate for all channels
2016 Antarctica DC8		MCoRDS 3 on DC8
2017 Greenland P3		MCoRDS 3 on P3 Tx power: 1050W
2017 Antarctica P3		MCoRDS 3 on P3 Tx power: 1050W
2017 Antarctica Basler		MCoRDS 5 on Airtech Basler Power amplifiers match 2013 Antarctica Basler Bandwidth: 150-450 MHz Tx power: 1800 W (225W per channel) Waveform: Eight channel chirp generation Acquisition: 8 channels, 12 bit ADC at 1600 MHz sampling Dynamic Range: waveform playlist Rx Aperture: Single 3.7 m array with 8 channels Tx Aperture: Same as Rx Monostatic tx/rx Data rate: 750 MB/sec aggregate for all channels
2018 Greenland P3		MCoRDS 3 on P3 Tx power: 337W Second from left element damaged. Only used right five elements for transmit. Left/right 15 deg beam steering used with Hanning weighted beam.

2018 Antarctica DC8		MCoRDS 3 on DC8 The 6 th rx channel was ~30dB down
2019 Greenland P3		MCoRDS 3 on P3 Second from left element repaired. All seven elements available for transmit. Only the center elements are installed similar to 2013 Greenland P3. Left/right 18 deg beam steering used. Left beam formed with three left-most elements. Right beam formed with right-most elements. Transmit phase center separation between beams allows for additional cross-track resolution (i.e. similar to ping-pong operation). Boxcar weights on antenna elements.
2019 Antarctica GV		MCoRDS 3 on GV 236-254 MHz Tx power: 500 W per channel (2000 W total) Four cross-track element array. Boxcar weighted beam. Monostatic tx/rx

Dynamic Range

The signal from the ice surface is typically much larger than the signal from the ice bottom. This is because of the attenuation of RF signals in ice. Generally speaking this requires that different receiver gains are used to capture these signals. Three methods have been used by the radar systems and are described here.

The sensitivity timing control (STC) is a fast-time gain control where the receiver gain is modified in real-time as the echoes are received. The original sensitivity timing control used a hand dial to control the STC and the STC was analog (not discrete). Radiometric calibration of the data is nearly impossible with these datasets.

Low and high gain channels means that two separate recordings of the data are made: one with low receiver gain and one with high receiver gain. It provides the most flexible and best quality dynamic range, but generally doubles the data rate and much of the hardware must be duplicated to capture two channels.

A waveform playlist allows low and high gain channels to be multiplexed in time. The idea is that the low gain channel typically requires fewer integrations to be useful and so only a small penalty is paid for time multiplexing (if time was split equally it would be 3 dB, but typical configurations lose less than 1 dB of sensitivity). The second idea is that two waveforms, one with a short pulse duration and one with a long pulse duration generally provide better coverage than a single pulse duration. The short pulse duration is used for close in targets that typically do not require high sensitivity and so this waveform doubles as the low gain channel and effectively no penalty is paid for time multiplexing the gain settings. For example, a waveform with a 1-µs duration and lower receiver gain settings is used to measure the round-trip signal time for the ice surface echo, while a waveform with a 10-µs duration and higher receiver gain settings is used to measure the round-trip signal time for the ice bottom echo. As stated above, the two different waveforms are used because of the large dynamic range of signal powers that are observed. The 10-µs duration and higher receiver gain settings are more sensitive to the bottom echo, but the signal is generally saturated and unusable from the ice surface and upper internal layers.

For high altitude data, the difference in power between the ice surface and ice bottom is small enough that a single high gain setting is possible.

Ice Thickness (also Ice Surface and Ice Bottom)

Ice thickness is typically determined using data collected from waveforms with different pulse durations. Generally all receive channels are used to produce the best result. The difference in the propagation time between the ice surface and ice bottom reflections is then converted into ice thickness using an estimated ice index of refraction of ice (square root of 3.15). The media is assumed to be uniform, i.e. no firn correction is applied.

L1B Processing Steps

The following processing steps are performed for CSARP products

1. Conversion from quantization to voltage at the 50 ohm antenna
2. Removal of DC-bias by subtracting the mean from each record
3. Channel compensation between each of the antenna phase centers. This includes time delay, amplitude, and phase mismatches. The channel equalization coefficients are found by monitoring the relative returns from each channel from the ocean surface at high altitude, smooth bed returns, and deep internal layers.
4. Pulse compression with time and frequency domain windows. Before 2009 Antarctica DC8, the transmitted pulse had a boxcar window. From 2009 Antarctica DC8 and forward, all transmitted pulses typically have a 20% Tukey window applied in the time domain. The matched filter applied to the received signal is identical to the transmitted waveform (typically an ideal transmission is assumed without system distortion) with a frequency domain window applied. The frequency domain window is usually a boxcar or hanning window.
5. For qlook and csarp-combined, every receiver channel used in the data product (which may not be all channels) are averaged together coherently. This is equivalent to beam-forming with the beam pointing towards nadir.
6. Motion compensation for attitude and trajectory lever arm (qlook and csarp-combined do not include motion compensation).
7. SAR processing with along-track spatial frequency window using f-k migration. Qlook product just uses presumming (aka stacking, unfocused SAR processing, or coherent averaging). The quick look output is used to find the ice surface location (fully automated) by using a maximum power layer tracker. This ice surface location is used to generate the dielectric model used by the SAR processing algorithms. The dielectric model for f-k migration is always a layered media with variation in the z-axis only.
8. Channel combination. Currently, channel combination usually combines channels within a sub-array. Qlook and csarp-combined combine channels before SAR processing so this step does not apply to these data products. Standard applies a normalized array window

before summing channels. MVDR uses the minimum variance distortionless response algorithm for channel combination and the spatial correlation matrix is estimated from a neighborhood of pixels surrounding the image pixel being combined. Channel combination also includes multi-looking or spatial incoherent (power) averaging followed by along-track decimation.

9. Waveform combination. Echograms from low and high gain channels are combined to form a single image. Generally combination is done T_{pd} seconds after the surface return where T_{pd} is the pulse duration of the transmitted chirp. This is because the surface return is often saturated in the high gain channel.

L2 Processing Steps

The layer tracking of ice surface and ice bottom reflections are manually driven processes with basic tools for partial automation. The tools used are determined by the operator picking the data and include:

1. manual picking and interpolation
2. snake tracker which follows the strongest return within a window centered on the last tracked location from range line to range line
3. leading edge detector which searches for the crossing of a threshold beneath the peak return
4. peak detector

Different processing outputs (e.g. mvdr, standard, qlook), dynamic range of the image, averaging, and detrending methods are used to better highlight features in the echogram as needed.

The primary error sources for ice penetrating radar data are system electronic noise, multiple reflectors, also known as multiples, and off-nadir reflections. All of these can create spurious reflections in the trace data leading to false echo layers in profile data.

Multiple reflectors arise when the radar energy reflects off two surfaces more than once (or resonates) in the vertical dimension, and then returns to the receive antenna. They occur in situations when two or more large reflectors are present with large electromagnetic constitutive property changes, such as the ice surface (air/ground), the bottom of the ice, and the aircraft body which is also a strong reflector. The radar receiver only records time since the radar pulse was emitted, so the radar energy that traveled the additional path length appears later in time, apparently deeper in the ice or even below the ice-bedrock interface. Note that multiples of a strong continuous reflector have a similar shape because the propagation time is a multiple of the resonance cavity. The most common multiple is between the air-ice surface and the aircraft. This “surface” multiple shows up at twice the propagation time as the original surface return and all the slopes are doubled.

Off-nadir reflections can result from crevassed surfaces, water, rock outcrops, or metal structures. Antenna beam structure and processing of the data are designed to reduce these off-nadir reflected energy sources.

L3 Processing Steps

The gridding process varies because of differing methods and data sources and is explained in the README file included with each grid.

Matlab Example to Load L1B and L2 Data

```
echogram_fn = 'E:\rds\2012_Greenland_P3\CSARP_standard\20120514_01\Data_20120514_01_014.mat';
layer_fn = 'E:\rds\2012_Greenland_P3\CSARP_layerData\20120514_01\Data_20120514_01_014.mat';

close all
echo = load(echogram_fn,'Data','Time','GPS_time');

h_fig = figure;
h_axes = axes;
imagesc(lp(echo.Data),'parent',h_axes);
colormap(h_axes,1-gray(256));
xlabel('Range line','parent',h_axes);
ylabel('Range bin','parent',h_axes);

layer = load(layer_fn,'GPS_time','layerData');
Surface =
interp1(echo.Time,1:length(echo.Time),layer.layerData{1}.value{2}.data);
Bottom =
interp1(echo.Time,1:length(echo.Time),layer.layerData{2}.value{2}.data);
Surface = interp1(layer.GPS_time,Surface,echo.GPS_time);
Bottom = interp1(layer.GPS_time,Bottom,echo.GPS_time);

hold(h_axes,'on');
plot(Surface,'m--','parent',h_axes);
plot(Bottom,'r--','parent',h_axes);
hold(h_axes,'off');
```

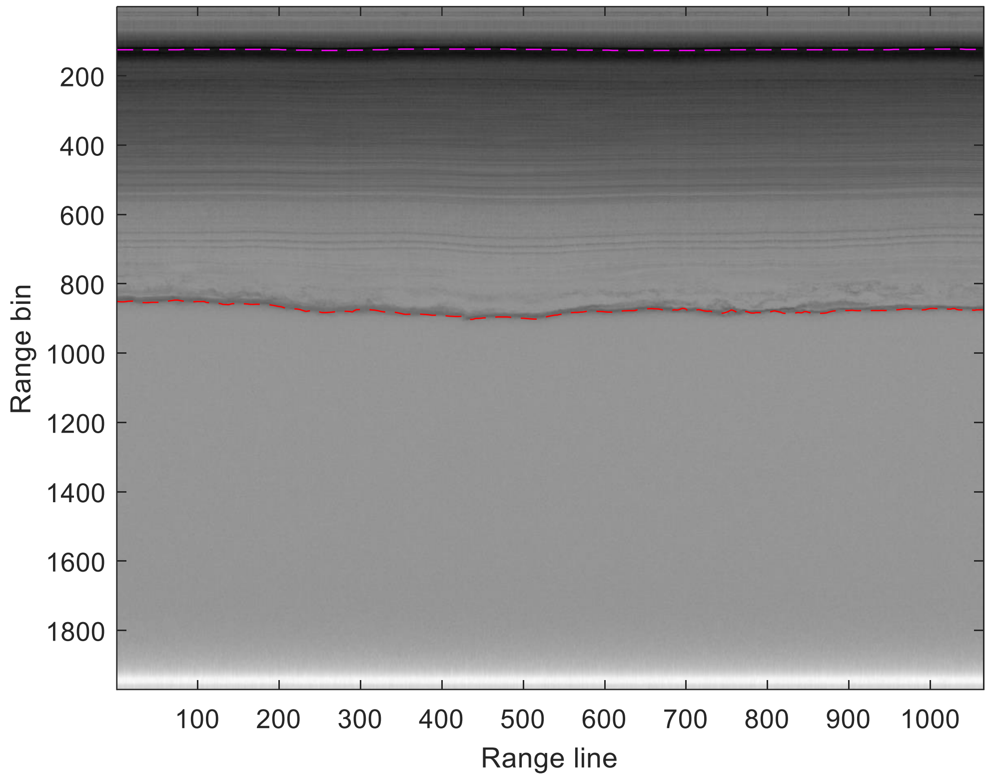

Resolution and Error Bounds

The range resolution, defined here as the minimum range difference to distinguish the return power from two targets with 16 dB of isolation, is determined as

$$\frac{k_t c}{2B\sqrt{3.15}},$$

where B is the bandwidth, 3.15 is the approximate dielectric of ice, c is the speed of light in a vacuum, and k_t is the window widening factor which is 0.88 for no windowing and 1.53 for 20% Tukey time-domain window on transmit followed by pulse compression with a similarly weighted Tukey time-domain window with a hanning frequency-domain window. The window widening factor was computed numerically and is the width of the pulse 3 dB down from the peak. Windowing is applied to improve the isolation between targets at different ranges, but causes the resolution to become worst. This table gives the range resolution for several bandwidths.

Bandwidth (MHz)	Range Resolution w/o windowing (m)	Range Resolution w/ windowing (m)
9.5	7.8	13.6
10	7.4	12.9
17.5	4.2	7.4
20	3.7	6.5
30	2.5	4.3
150	0.5	0.9
180	0.4	0.7

If there is only one target, the range accuracy to that one target is dependent on the signal to noise ratio (SNR), and is given by

$$\frac{k_t c}{2\mathrm{B}\sqrt{3.15}\sqrt{2 \cdot \mathrm{SNR}}}.$$

The table below repeats the above table with an SNR of 20 dB.

Bandwidth (MHz)	Range Resolution w/o windowing (m)	Range Accuracy w/ windowing (m)
9.5	0.55	0.96
10	0.53	0.91
17.5	0.30	0.52
20	0.26	0.46
30	0.18	0.30
150	0.04	0.06
180	0.03	0.05

The along-track resolution depends on the processing. The default processing parameters since Jan 1, 2011 are described here. For the single look complex (SLC) SAR-processed image (not quick look), the synthetic beamwidth is β_x = 10 deg and the along-track resolution is approximately:

$$\sigma_{x,SLC} = \frac{\lambda}{2\beta_x} k_x = 4.8\,\mathrm{m},$$

where k_x = 1.1 is the along-track windowing factor for a 20% tukey window. The SLC produced by the processing is over-sampled by a factor of approximately 2 and the final product has 11 along-track looks and 1 range look and is then decimated by 6. Therefore, the final product has an along-track resolution of about σ_x = 25 m and a sample spacing of about 14 m.

While the range and along-track position are known with fine resolution, the cross-track resolution is poor. For a rough surface, the off-nadir echoes can mask the nadir echo and an off-nadir return may be selected as the ice bottom rather than the nadir return. The best case is to have crossovers in the dataset so you can estimate the precision of the ice bottom layer picks.

For a smooth surface with no appreciable roughness, the cross-track resolution will be constrained to the first Fresnel zone, which is approximately

$$\sigma_{y,\text{Fresnel-limited}} = \sqrt{2\left(H + T/\sqrt{3.15}\right)\lambda_c}\ ,$$

where H is the height above the air/ice interface, T is the ice thickness, and λ_c is the wavelength at the center frequency. The table below gives the cross-track resolution for several different parameters.

Center Frequency (MHz)	**Cross-track Resolution H = 500 m T = 2000 m (m)**	**Cross-track Resolution H = 8000 m T = 2000 m (m)**
125	88.3	209.2
150	80.6	191.0
195	70.7	167.5
210	68.2	161.4

For a rough surface with no appreciable layover, the cross-track resolution will be constrained by the pulse-limited footprint, which is approximately

$$\sigma_{y,\text{pulse-limited}} = 2\sqrt{\frac{\left(H + T/\sqrt{3.15}\right)ck_t}{B}}\ .$$

The table below gives the cross-track resolution with windowing.

Bandwidth (MHz)	**Cross-track Resolution H = 500 m T = 2000 m (m)**	**Cross-track Resolution H = 500 m T = 8000 m (m)**
9.5	561	1328
10	546	1294
17.5	413	978
20	386	915
30	315	747
150	141	334
180	129	305

For a rough surface where layover occurs, the cross-track resolution is set by the beamwidth, β_y, of the antenna array. The antenna beamwidth is approximately:

$$\beta_y = \sin^{-1}\frac{\lambda_c}{Nd_y},$$

where N is the number of elements, and d_y is the element spacing. The table below gives the beamwidth for the various platforms.

Platform	N	d_y (λ_c)	**Beamwidth (deg)**
P-3 original	4	0.5	30.0
TO	4	0.5	30.0
TO	5	0.5	23.6
TO	6	0.5	19.5
P-3 new (center-array only)	7	0.5	16.6
DC-8	5	0.25	53.1

The antenna beamwidth-limited resolution is

$$\sigma_{y,\text{beamwidth-limited}} = 2\left(H + \frac{T}{\sqrt{3.15}}\right)\tan\left(\frac{\beta_y k_y}{2}\right)$$

where β_y is in radians and k_y = 1.3 is the approximate cross-track windowing factor for a hanning window applied to a small cross-track antenna array.

Platform	N	d_y (λ_c)	**Cross-track Resolution H = 500 m T = 2000 m (m)**	**Cross-track Resolution H = 500 m T = 8000 m (m)**
P-3 original	4	0.5	1152	3546
TO	4	0.5	1152	3546
TO	5	0.5	893	2747
TO	6	0.5	732	2252
P-3 new (center-array only)	7	0.5	620	1909
DC-8	5	0.25	2237	6887

The dielectric error is expected to be on the order of 1% for typical dry ice (Fujita et al) and no compensation has been done for a firn layer in SAR processing where the ice is treated as a homogeneous medium with a dielectric of 3.15. The dielectric error using the first term of the Taylor series creates an ice thickness dependent error given by:

$$\Delta T = \frac{-T}{2}\varepsilon_{\%\text{error}} = \frac{-T}{200}$$

So for an ice thickness of T = 2000, a 1% dielectric error creates a 10 m thickness error.

The system loop sensitivity is the SNR with no channel losses (spreading loss, extinction, and backscattering) which is

$$SNR = \frac{P_t (N_c G \lambda_c)^2 N_{ave} B T_{pd}}{4\pi k T B F \cdot \mathrm{m}^2}$$

where P_t is the total transmit power including system losses, N_c is the number of channels on transmit and receive used in echogram formation, G is the individual antenna element accounting for the ground plane, N_{ave} is the approximate number of pulses that may be averaged in SAR processing and presumming, T_{pd} is the pulse duration, λ_c is the wavelength at the center frequency, k = 1.38e-23 WsK^{-1} is Boltzmann's constant, T = 290 K is the approximated noise temperature before the receiver, $F = 2$ is the approximate noise figure of the receiver, and m^2 is 1 meter squared to cancel out units.

Platform	P_t	N_c	G	N_{ave}	T_{pd} (µs)	λ_c (m)	**Loop Sensitivity (dB)**
ICARDS P-3	25	4	4		1.6	2	
ICARDS2 P-3	25	4	4		1.6	2	
ACORDS P-3	25	4	4		3	2	
ACORDS TO	40	5	4		3	2	
WCORDS Ground	50	4	1		10	2.4	
SAR Ground	800	[1 8]	4		10	1.43	
MCRDS TO (4 elements)	200	4	4		10	2	
MCRDS TO (5 elements)	160	5	4		10	2	
MCRDS TO (6 elements)	133	6	4		10	2	
MCRDS P-3	200	4	4		10	2	
MCRDS Ground		[1 8]			10	2	
MCORDS DC-8	300	5	1	3200	10	1.54	220
MCORDS P-3	166	7	4	3200	10	1.54	230
MCORDS TO (150 MHz)	300	6	4	3200	10	2	233
MCORDS TO	300	6	4	3200	10	1.54	231
MCORDS2 P-3	300	7	4	3200	10	1.54	231
MCORDS2 TO	300	6	4	3200	10	1.54	231
MCORDS2 DC8	300	5	4	3200	10	1.54	231

Ice Bottom Error Analysis

We recommend using one of two methods for performing the error analysis. One method is to take the RMS error of the range resolution of the system and add in the RMS error of the dielectric. This assumes that the error in the ice surface elevation is zero. The ice surface location is important because it determines where the dielectric changes from 1 to 3.15 and therefore affects the radar time to radar range conversion. However, since the surface is usually well detected and flat, the RMS error of the surface may be very small as long as system time delay biases are removed properly. Each of the RMS errors are described in the preceding section and the general equation is:

$$RMS = \left(\left(\frac{k_t c}{2B\sqrt{3.15}} \right)^2 + \left(\frac{-T}{200} \right)^2 \right)^{0.5}$$

where

k_t is the window widening factor (1.53)

c is the speed of light in a vacuum

B is the waveform bandwidth (e.g. 9.5 MHz for 2010 Greenland DC8)

T is the ice thickness.

Another method is to use cross over analysis and compute the RMS differences in ice bottom elevation between nearby crossing lines and add the RMS error of the dielectric to that:

$$RMS = \left((crossovers)^2 + \left(\frac{-T}{200} \right)^2 \right)^{0.5}$$

The first method is probably the most accurate for flat terrain where the ice bottom interface is unambiguous and cross track resolution is not important. The second method, based on the cross over analysis, may be more reasonable for complex ice bottom terrains and provide a more accurate estimate of the error.

Season Specific Information

All of the data are not radiometrically calibrated. This means that they are not converted to some absolute standard for reflectivity or backscattering analysis. We are working on data processing and hardware modifications to do this.

1993 Greenland P3 (NASA)

While these data are in the new format, they were processed through an older set of code. The fast-time origin (Time variable) is not calibrated so that the data products only have valid thickness data because the surface and bottom information has an unknown offset. Radar and data processing settings are also not included in the files.

This section is not completed.

1995 Greenland P3 (NASA)

While these data are in the new format, they were processed through an older set of code. The fast-time origin (Time variable) is not calibrated so that the data products only have valid thickness data because the surface and bottom information has an unknown offset. Radar and data processing settings are also not included in the files.

This section is not completed.

1996 Greenland P3 (NASA)

While these data are in the new format, they were processed through an older set of code. The fast-time origin (Time variable) is not calibrated so that the data products only have valid thickness data because the surface and bottom information has an unknown offset. Radar and data processing settings are also not included in the files.

This section is not completed.

1997 Greenland P3 (NASA)

While these data are in the new format, they were processed through an older set of code. The fast-time origin (Time variable) is not calibrated so that the data products only have valid thickness data because the surface and bottom information has an unknown offset. Radar and data processing settings are also not included in the files.

This section is not completed.

1998 Greenland P3 (NASA)

While these data are in the new format, they were processed through an older set of code. The fast-time origin (Time variable) is not calibrated so that the data products only have valid thickness data because the surface and bottom information has an unknown offset. Radar and data processing settings are also not included in the files.

This section is not completed.

1999 Greenland P3 (NASA)

While these data are in the new format, they were processed through an older set of code. The fast-time origin (Time variable) is not calibrated so that the data products only have valid thickness data because the surface and bottom information has an unknown offset. Radar and data processing settings are also not included in the files.

This section is not completed.

2001 Greenland P3 (NASA)

While these data are in the new format, they were processed through an older set of code. The fast-time origin (Time variable) is not calibrated so that the data products only have valid thickness data because the surface and bottom information has an unknown offset. Radar and data processing settings are also not included in the files.

This section is not completed.

2002 Greenland P3 (NASA)

While these data are in the new format, they were processed through an older set of code. The fast-time origin (Time variable) is not calibrated so that the data products only have valid thickness data because the surface and bottom information has an unknown offset. Radar and data processing settings are also not included in the files.

This section is not completed.

2002 Antarctica P3chile (NASA)

While these data are in the new format, they were processed through an older set of code. The fast-time origin (Time variable) is not calibrated so that the data products only have valid thickness data because the surface and bottom information has an unknown offset. Radar and data processing settings are also not included in the files.

This section is not completed.

2003 Greenland Ground (NSF)

While these data are in the new format, they were processed through an older set of code. The fast-time origin (Time variable) is not calibrated so that the data products only have valid thickness data because the surface and bottom information has an unknown offset. Radar and data processing settings are also not included in the files.

This section is not completed.

2004 Antarctica P3chile (NASA)

While these data are in the new format, they were processed through an older set of code. The fast-time origin (Time variable) is not calibrated so that the data products only have valid thickness data because the surface and bottom information has an unknown offset. Radar and data processing settings are also not included in the files.

This section is not completed.

2005 Greenland Ground (NSF)

These data were taken around summit with a 120-300 MHz broadband system with an 8 channel cross-track array. The data are not currently available. Processing these data into the new format is not currently on the schedule.

2005 Greenland TO (NASA)

While these data are in the new format, they were processed through an older set of code. The fast-time origin (Time variable) is not calibrated so that the data products only have valid thickness data because the surface and bottom information has an unknown offset. Radar and data processing settings are also not included in the files.

This section is not completed.

2005 Antarctica GPRWAIS (NSF)

These data were taken around WAIS camp with a 140-160 MHz system with an 8 channel cross-track array.

While these data are in the new format, they were processed through an older set of code. The fast-time origin (Time variable) is not calibrated so that the data products only have valid thickness data because the surface and bottom information has an unknown offset. Radar and data processing settings are also not included in the files.

2006 Greenland Ground (?)

These data are only available in the old format because we are working on a raw file format problem. They are from Flade Raw in northeast Greenland. Processing these data into the new format is not currently on the schedule.

2006 Greenland TO (NASA and NSF)

While these data are in the new format, they were processed through an older set of code. The fast-time origin (Time variable) is not calibrated so that the data products only have valid thickness data because the surface and bottom information has an unknown offset. Radar and data processing settings are also not included in the files.

This section is not completed.

Field Team

Principle Investigator: Prasad Gogineni
Radar Installation: Torry Akins, Pannirselvam Kanagaratnam, Adam Lohoefener, John Paden
Radar Operation: Pannirselvam Kanagaratnam
Data Processing: NA
Data Backups and IT: NA
Post Data Processing (for this release): Jilu Li, John Paden, Weibo Liu, Logan Smith, Qi Shi, Abbey Whisler, Joe Lilek, Stephen Yan

2007 Greenland Ground (NSF)

These data are not currently available. This was a traverse from NGRIP to NEEM from July 17 to August 8 and includes some data at the ice cores as well.

This section is not completed.

2007 Greenland P3 (NASA and NSF)

While these data are in the new format, they were processed through an older set of code. The fast-time origin (Time variable) is not calibrated so that the data products only have valid thickness data because the surface and bottom information has an unknown offset. Radar and data processing settings are also not included in the files.

This section is not completed.

Field Team

Principle Investigator: Prasad Gogineni
Radar Installation:
Radar Operation: Fernando Rodriguez
Data Processing:
Data Backups and IT:
Post Data Processing (for this release):

2008 Greenland Ground (NSF)

These data are from NEEM camp.

This section is not completed.

2008 Greenland TO (NASA and NSF)

These data are only available in the old format. We are currently reprocessing these data into the new format with an expected ready date of Dec 2011.

Field Team

Principle Investigator: Prasad Gogineni
Radar Installation:
Radar Operation: Fernando Rodriguez
Data Processing:
Data Backups and IT:
Post Data Processing (for this release): Jilu Li, John Paden, Weibo Liu, Logan Smith, Qi Shi, Abbey Whisler, Joe Lilek, Stephen Yan

2008 Greenland Gambit (NSF)

The data are not currently available. Processing these data into the new format is not currently on the schedule.

2008 Antarctica Gambit (NSF)

The data are not currently available. We are currently reprocessing these data into the new format with an expected ready date of Dec 2011.

2008 Antarctica Ground (NSF)

The data are not currently available. We are currently reprocessing these data into the new format with an expected ready date of Dec 2011.

2009 Greenland TO (NSF)

These data are only available in the old format. We are currently reprocessing these data into the new format with an expected ready date of Dec 2011.

No coincident LIDAR data are available for this season.

Field Team

Principle Investigator: Prasad Gogineni
Radar Installation:
Radar Operation: Fernando Rodriguez
Data Processing:
Data Backups and IT:
Post Data Processing (for this release): Jilu Li, John Paden, Weibo Liu, Logan Smith, Qi Shi, Abbey Whisler, Joe Lilek, Stephen Yan

2009 Antarctica DC8 (NASA)

Known Issues

Transmit/Receive Switch: During the first two field seasons (2009 Antarctica DC-8 and 2010 Greenland DC-8), extra antennas inside the cabin were used to detect the ice surface delay time because the TR switches did not meet their switching time specification. As a side note, the extra antennas were originally installed to measure the electromagnetic interference environment and not the ice surface.

Some of the data collected during this season are from high altitude. The high altitude data are generally lower quality than the low altitude data. This is because:

1. The cross-track antenna resolution is proportional to range creating severe layover problems in mountainous terrain, for example 05 November 2009 high altitude peninsula flight.
2. The sidelobes from the long pulse duration mask out some of the returns that otherwise would have had a high enough signal to noise ratio.
3. The range to target is greater so the spherical spreading power loss is greater leading to a lower signal to noise ratio.

Monostatic elements: All monostatic elements used for transmit and receive have an unknown fast-time gain profile because the transmit/receive switches take about 10 microseconds to fully switch positions. This fast-time gain profile has not been corrected so that using the surface or shallow layer returns for antenna equalization or for radiometric purposes is not recommended. All five of the antennas are monostatic antennas on the DC-8.

Field Team

Principle Investigator: Christopher Allen
Radar Installation: Christopher Allen, Lei Shi, Ben Panzer, Rick Hale, Emily Arnold, John Hunter
Radar Operation: Lei Shi, Ben Panzer, William Blake, Victor Jara-Olivares, Christopher Allen
Data Processing: William Blake, Keith Lehigh, Ben Panzer, Lei Shi
Data Backups and IT: Keith Lehigh, Ben Panzer, Lei Shi
Post Data Processing (for this release): Hilary Barbour, William Blake, Steven Foga, Julia Guard, Anthony Hoch, Shashanka Jagarlapudi, Brady Maasen, John Paden, Kyle Purdon, Logan Smith, Theresa Stumpf

2009 Antarctica TO (NSF)

Known Issues

Field Team

Principle Investigator: Prasad Gogineni
Radar Operation: Carl Leuschen, Fernando Rodriguez
Data Processing: Logan Smith

2010 Greenland DC8 (NASA)

Known Issues

Transmit/Receive Switch: See 2009 Antarctica DC8.

High altitude data: See 2009 Antarctica DC8

Monostatic elements: See 2009 Antarctica DC8

Field Team

Principle Investigator: Carl Leuschen
Radar Installation: Reid Crowe, Ben Panzer, Fernando Rodriguez-Morales
Radar Operation: Reid Crowe, Ben Panzer, Fernando Rodriguez-Morales
Data Processing: Ben Panzer, Fernando Rodriguez-Morales, Jenett Tillotson
Data Backups and IT: Jenett Tillotson
Post Data Processing (for this release): Hillary Barbour, Steven Foga, Anthony Hoch, Shashanka Jagarlapudi, Brady Maasen, John Paden, Kyle Purdon, Logan Smith

2010 Greenland P3 (NASA)

Known Issues

Monostatic elements: See 2009 Antarctica DC8. Only the center seven elements are monostatic on the P-3.

EMI: Due to lack of shielding, a noisy switching power supply, and potentially other unidentified sources the radar was operated with 10 MHz bandwidth (190-200 MHz) for most of the field season. The signal quality is still lower than expected in this band due to broadband noise which is present at all times and periodic burst noise from other pulsed instruments on the P-3 and from random burst noise. The noise present at all times manifests itself as an increase in the noise floor and the burst noise manifests itself as smeared point targets.

Transmit/Receive Switch: This is a similar problem as with the 2009 Antarctica DC8 season (so see that section). However, we were able to set the TR switch control signals so that the surface is recoverable with the regular array down to an altitude of 600 ft AGL but with very much reduced signal strength. The regular array is preferred over the EMI antenna setup because the radiation pattern characteristics are better. At an altitude of 1500 ft, no degradation in signal detectability is observed. Note: the TR switches still do not switch quickly enough and affect the radiometric accuracy for about 10 microseconds after the switching event. This causes the receiver gain to be a function of time similar to a sensitivity timing control. This varying receiver gain is not compensated during processing.

Field Team

Principle Investigator: Carl Leuschen
Radar Installation: Emily Arnold, Kyle Byers, Reid Crowe, Richard Hale, John Hunter, Carl Leuschen, Fernando Rodriguez-Morales, Dennis Sundermeyer
Radar Operation: Kyle Byers, Fernando Rodriguez-Morales
Data Processing: Kyle Byers, Carl Leuschen, John Paden
Data Backups and IT: Chad Brown
Post Data Processing (for this release): Hillary Barbour, Aric Beaver, Steven Foga, Shashanka Jagarlapudi, Brady Maasen, John Paden, Kyle Purdon

2010 Antarctica DC8 (NASA)

Known Issues

High altitude data: See 2009 Antarctica DC8

Monostatic elements: See 2009 Antarctica DC8

T/R Switch: See 2010 Greenland P3

Field Team

Principle Investigator: Carl Leuschen
Radar Installation: Austin Arnett, Carl Leuschen, John Paden, Ben Panzer, Fernando Rodriguez-Morales
Radar Operation: Daniel Gomez, John Paden, Fernando Rodriguez-Morales
Data Processing: Carl Leuschen, John Paden
Data Backups and IT: Chad Brown, Dan Hellebust
Post Data Processing (for this release): Aric Beaver, Steven Foga, Shashanka Jagarlapudi, Jilu Li, Brady Maasen, John Paden, Kyle Purdon

2011 Greenland P3 (NASA)

Known Issues

The mcords2 data acquisition system, fielded for the first time this season, had a known issue this season with radar data synchronization with GPS data. The synchronization time correction that must be added to the radar time stamp is either 0 or -1 seconds. When the radar system is initially turned on, the radar system acquires UTC time from the GPS NMEA string. If this is done too soon after the GPS receiver has been turned on, the NMEA string sometimes returns GPS time rather than UTC time. GPS time is 15 seconds ahead of UTC time during this field season. The corrections for all segments affected by this must include the offset and are -15 or -16 seconds.

GPS corrections have been applied to all of the data using a comparison between the accumulation radar and the MCoRDS radar. The accumulation radar from this season is known to have only the GPS/UTC problem. The GPS/UTC problem is easily detectable by comparing the data to raster imagery, so the only correction that could be in error is the 0 or -1 second offset and this generally happens when there are no good features in or above the ice to align the accumulation and mcords2 radars. The GPS time corrections that were applied and the segments where no good sync information was available are given in the vector worksheet of the parameter spreadsheet. This issue is closed.

Two of the missions (SE Glaciers on Apr 11 and Helheim/Kanger/Midguard on Apr 19) suffered from radar configuration failures and we lost about 40 dB of sensitivity on the high gain channel. Short portions of these data are still good so the datasets were published, but most of the data are not useful. We believe at this point that no recovery is possible. This issue is closed.

High altitude data: See 2009 Antarctica DC8

Monostatic elements: See 2009 Antarctica DC8. Only the center seven elements are monostatic on the P-3.

T/R Switch: See 2010 Greenland P3

Field Team

Principle Investigator: Carl Leuschen
Radar Installation: Emily Arnold, Kyle Byers, Reid Crowe, Richard Hale, John Hunter, Carl Leuschen, John Paden, Ben Panzer, Kevin Player, Fernando Rodriguez-Morales
Radar Operation: Austin Arnett, Carl Leuschen, John Paden, Kevin Player
Data Processing: John Paden
Data Backups and IT: Dan Hellebust, Justin Miller
Post Data Processing (for this release): Hillary Barbour, Aric Beaver, Steven Foga, Jilu Li, Brady Maasen, John Paden, Kyle Purdon

Release Dates

Release 2.0 of L1B and L2 data was Oct 20, 2011.

Expected 3.0 release of L1B, L2, and L3 data is Jan 20, 2011.

2011 Greenland TO (NSF)

Data processing not completed.

No coincident LIDAR data are available for this season.

High speed GaNi/hybrid transmit receive switches with circulator installed with 100 ns switching time. This fixes the TR switching time problem described in 2009 Antarctica DC8 and 2010 Greenland P3.

Field Team

Principle Investigator: Prasad Gogineni
Radar Installation: Reid Crowe, Fernando Rodriguez
Radar Operation: Daniel Gomez, Fernando Rodriguez
Data Processing: Logan Smith
Data Backups and IT: Chad Brown
Post Data Processing (for this release):

2011 Antarctica DC8 (NASA)

High altitude data: See 2009 Antarctica DC8

Monostatic elements: See 2009 Antarctica DC8

T/R Switch: See 2010 Greenland P3

Field Team

Principle Investigator: Carl Leuschen
Radar Installation: Austin Arnett, Jilu Li, John Paden, Ben Panzer, Kevin Player
Radar Operation: John Paden
Data Processing: Shashanka Jagarlapudi, John Paden
Data Backups and IT: Matt Standish
Post Data Processing (for this release): Shashanka Jagarlapudi, John Paden, Kyle Purdon, Steven Foga, John King, Sam Buchanan

2011 Antarctica TO (NSF)

This field season concentrated on Byrd Glacier and its catchment area. No high altitude data were collected.

No coincident LIDAR data are available for this season.

High speed GaNi/hybrid transmit receive switches with circulator installed with 100 ns switching time. This fixes the TR switching time problem described in 2009 Antarctica DC8.

Monostatic elements: See 2009 Antarctica DC8. Half the receive channels are monostatic.

Field Team

Principle Investigator: Prasad Gogineni
Radar Installation: Reid Crowe, Daniel Gomez, Fernando Rodriguez-Morales
Radar Operation: Reid Crowe, Fernando Rodriguez-Morales
Data Processing: Jilu Li
Data Backups and IT: Justin Miller
Post Data Processing (for this release): Jilu Li, Thersa Stumpf, John Paden, Kyle Purdon,

2012 Greenland P3 (NASA)

High altitude data: See 2009 Antarctica DC8

Monostatic elements: See 2009 Antarctica DC8. Only the center seven elements are monostatic on the P-3.

T/R Switch: See 2010 Greenland P3

Field Team

Principle Investigator: Carl Leuschen
Radar Installation: Aqsa Patel, Kevin Player
Radar Operation: Carl Leuschen, John Paden, Kevin Player
Data Processing: John Paden, Logan Smith, Theresa Stumpf
Data Backups and IT: Erik Cornet, Justin Miller, Matt Standish
Post Data Processing (for this release): John King, Kyle Purdon, Logan Smith, Trey Stafford, Theresa Stumpf

2012 Antarctica DC8 (NASA)

High altitude data: See 2009 Antarctica DC8

Monostatic elements: See 2009 Antarctica DC8. Only the center seven elements are monostatic on the P-3.

High speed GaNi/hybrid transmit receive switches with circulator installed with 100 ns switching time. This fixes the TR switching time problem described in 2009 Antarctica DC8 and 2010 Greenland P3.

Field Team

Principle Investigator: Carl Leuschen
Radar Installation: Fernando Rodriguez, Bryan Townley
Radar Operation: John Paden
Data Processing: John Paden, Isaac Tan
Data Backups and IT: Carson Gee, Matt Standish
Post Data Processing (for this release): Sam Buchanan, John King, John Paden, Kyle Purdon, Trey Stafford, Isaac Tan, Haiji Wang, Zengxin Zhang

2013 Greenland P3 (NASA)

Only the center 7 antenna elements were installed to reduce costs.

High altitude data: See 2009 Antarctica DC8

Monostatic elements: See 2009 Antarctica DC8. Only the center seven elements are monostatic on the P-3.

Field Team

Principle Investigator: Carl Leuschen
Radar Installation: Fernando Rodriguez, Bryan Townley

Radar Operation: John Paden, Bruno Camps-Raga, Bryan Townley
Data Processing: John Paden, Logan Smith, Theresa Stumpf
Data Backups and IT: Matt Standish, Aaron Wells, and others
Post Data Processing (for this release): Sam Buchanan, John King, John Paden, Kyle Purdon, Trey Stafford, Isaac Tan, Haiji Wang, Zengxin Zhang

2013 Antarctica P3 (NASA)

High altitude data: See 2009 Antarctica DC8

Monostatic elements: See 2009 Antarctica DC8. Only the center seven elements are monostatic on the P-3.

Field Team

Principle Investigator: Carl Leuschen
Radar Installation: Fernando Rodriguez, Bryan Townley
Radar Operation: Bruno Francisco Camps Raga, Bryan Townley
Data Processing: Theresa Stumpf
Data Backups and IT: Justin Miller
Post Data Processing (for this release): Jilu Li

2013 Antarctica Basler (NSF)

High altitude data: See 2009 Antarctica DC8

Monostatic elements: See 2009 Antarctica DC8. Only the center seven elements are monostatic on the P-3.

Field Team

Principle Investigator: Prasad Gogineni (STC) and Richard Hale (MRI)
Radar Installation: Carl Leuschen, John Paden, Fernando Rodriguez, Bryan Townley, Zongbo Wang
Radar Operation: John Paden, Zongbo Wang
Data Processing: John Paden
Data Backups and IT: Aaron Wells
Post Data Processing (for this release): John Paden

2014 Greenland P3 (NASA)

High altitude data: See 2009 Antarctica DC8

Monostatic elements: See 2009 Antarctica DC8. Only the center seven elements are monostatic on the P-3.

Field Team

Principle Investigator: Carl Leuschen
Radar Installation: Fernando Rodriguez, Bryan Townley
Radar Operation: Bruno Camps-Raga, Carl Leuschen, Bryan Townley

Data Processing: Jilu Li, John Paden
Data Backups and IT: Aaron Wells
Post Data Processing (for this release): Jilu Li

2014 Antarctica DC8 (NASA)

New antenna array installed. New power amplifiers (1800 W of power) and receivers installed to support 165-215 MHz bandwidth. New digital system sampling frequency to support new bandwidth.

High altitude data: See 2009 Antarctica DC8

Monostatic elements: See 2009 Antarctica DC8.

Field Team

Principle Investigator: Carl Leuschen
Radar Installation: Aaron Paden, Fernando Rodriguez, Bryan Townley
Radar Operation: Calen Lee Carabajal, Jay Fuller
Data Processing: Jilu Li, John Paden
Data Backups and IT: Aaron Wells
Post Data Processing (for this release): Jilu Li

2015 Greenland C130 (NASA)

New wideband antenna installed with 2 elements. New digital system installed. New transmitter and receiver installed to support 180-450 MHz bandwidth.

Small antenna aperture: The antenna aperture is very small with two very closely spaced elements and therefore the cross-track resolution is very coarse leading to higher clutter compared with other seasons.

High altitude data: See 2009 Antarctica DC8

Monostatic elements: See 2009 Antarctica DC8. Both elements are monostatic.

Field Team

Principle Investigator: Carl Leuschen
Radar Installation: Aaron Paden, Fernando Rodriguez, Bryan Townley
Radar Operation: Faiz Ahmed, John Paden, Bryan Townley
Data Processing: Jilu Li, John Paden
Data Backups and IT: Aaron Wells
Post Data Processing (for this release): Jilu Li

2015 Greenland Polar6 (NSF)

This was a test campaign for EMI certification, radar calibration and validation. A very limited number of flights were conducted (8 total) with only 3 collecting data over the ice sheets. No high altitude data were collected.

New wideband antenna installed with 24 elements. New digital system installed. New transmitter and receiver installed to support antenna and 150-600 MHz bandwidth. New power amplifiers support 6000 W of transmitted power.

Monostatic elements: See 2009 Antarctica DC8. Only the center fuselage array with 8 elements is monostatic.

Field Team

Principle Investigator: Richard Hale
Radar Installation: Aaron Paden, Fernando Rodriguez, Bryan Townley
Radar Operation: John Paden, Fernando Rodriguez
Data Processing: John Paden
Data Backups and IT: Riley Epperson
Post Data Processing (for this release): John Paden

2017 Greenland P3 (NASA)

High altitude data: See 2009 Antarctica DC8

Monostatic elements: See 2009 Antarctica DC8. Only the center seven elements are monostatic on the P-3.

Accumulation radar created noise on MCoRDS receivers. Solved by adding filters to accumulation radar transmit.

Science data system cables routed near MCoRDS center element cables caused elevated noise. Solved by improving routing and adding ferrite chokes to RF cables.

Added IMU-GPS measurements in each wing tip. Caused a small increase in noise on the right wing.

Field Team

Principle Investigator: Carl Leuschen
Radar Installation: Fernando Rodriguez, Bryan Townley
Radar Operation: John Paden, Bryan Townley
Data Processing: John Paden
Data Backups and IT: Aaron Wells
Post Data Processing (for this release):

Acknowledgement, Citing, and Reporting Data Use:

If you present or publish these data or results using the data, please help us with our record keeping by filling out the online form at http://data.cresis.ku.edu/.

To cite the data please use the following:

CReSIS. 2016. CReSIS Radar Depth Sounder Data, Lawrence, Kansas, USA. Digital Media. http://data.cresis.ku.edu/.

To acknowledge the use of the data, please use the following (all data products have been generated using tools generated with NSF funding so regardless of the season please acknowledge NSF's contribution):

We acknowledge the use of data and/or data products from CReSIS generated with support from the University of Kansas, NSF grant ANT-0424589, and NASA Operation IceBridge grant NNX16AH54G.

References and Related Publications

CReSIS Website (https://www.cresis.ku.edu/).

IceBridge Data Web site at NSIDC (http://nsidc.org/data/icebridge/index.html).

IceBridge Web site at NASA (http://www.nasa.gov/mission_pages/icebridge/index.html).

ICESat/GLAS Web site at NASA Wallops Flight Facility (http://glas.wff.nasa.gov/).

ICESat/GLAS Web site at NSIDC (http://nsidc.org/daac/projects/lidar/glas.html).

Akins, Torry Lee, "Design and development of an improved data acquisition system for the coherent radar depth sounder", Department of Electrical Engineering and Computer Science: Master's Thesis, University of Kansas, 1999.

Christopher Allen, Lei Shi , Richard Hale , Carl Leuschen , John Paden , Benjamin Panzer , Emily Arnold , William Blake , Fernando Rodriguez-Morales , John Ledford , Sarah Seguin, “Antarctic Ice Depth Sounding Radar Instrumentation for the NASA DC-8”, submitted for publication to IEEE Transactions on Aerospace and Electronic Systems, Aug 2011.

Blake, W.; Ledford, J.; Allen, C.; Leuschen, C.; Gogineni, S.; Rodriguez-Morales, F.; Lei Shi; , "A VHF Radar for Deployment on a UAV for Basal Imaging of Polar Ice," *Geoscience and Remote Sensing Symposium, 2008. IGARSS 2008. IEEE International* , vol.4, no., pp.IV-498-IV-501, 7-11 July 2008
doi: 10.1109/IGARSS.2008.4779767

Byers, K. J., "Integration of a 15-Element, VHF Bow-Tie Antenna Array into an Aerodynamic Fairing on a NASA P-3 Aircraft", Department of Electrical Engineering and Computer Science: Master's Thesis, University of Kansas, 06/2011.

Byers, Kyle J., A. R. Harish, Sarah A. Seguin, Carlton Leuschen, Fernando Rodriguez-Morales, John Paden, Emily Arnold and Richard Hale, “A Modified Wideband Dipole Antenna for an Airborne VHF Ice Penetrating Radar,” submitted to IEEE Transactions on Instrumentation and Measurement, June 2011.

Chuah, T. S., "Design and Development of a Coherent Radar Depth Sounder for Measurement of Greenland Ice Sheet Thickness", CReSIS Technical Report, no. 151, pp. 175, 01/1997.

Fujita, Shuji, Takeshi Matsuoka, Toshihiro Ishida, Kenichi Matsuoka, and Shinji Mae, “A summary of the complex dielectric permittivity of ice in the megahertz range and its application for radar sounding of polar ice sheets,” *Physics of Ice Core Records*, Edited by T. Hondoh, Hokkaido University Press, 2000, Sapporo, pp. 185-212.

Gogineni, S., T. Chuah, C. Allen, K. Jezek, R. K. Moore, “An improved coherent radar depth sounder,” Journal of Glaciology, vol. 44, no. 148, pp. 659-669, 1998.

Gogineni, S., D. Tammana, D. Braaten, C. Leuschen, T. Akins, J. Legarsky, P. Kanagaratnam, J. Stiles, C. Allen, and K. Jezek, "Coherent radar ice thickness measurements over the Greenland ice sheet", Journal of Geophysical Research-Atmospheres, vol. 106, no. D24, pp. 33761-33772, Dec, 2001.

Rick Hale, Heinrich Miller, Sivaprasad Gogineni, Jie-Bang Yan, Fernando Rodriguez-Morales, Carl Leuschen, John Paden, Jilu Li, Tobias Binder, Daniel Steinhage, Martin Gehrmann, David Braaten, Multi-channel Ultra-wideband radar sounder and imager, #3821, IGARSS 2016, 10-15 July 2016, Beijing, China.

Namburi, S. P. V., "Design and Development of an Advanced Coherent Radar Depth Sounder", Department of Electrical Engineering and Computer Science, Master's Thesis, University of Kansas, 2003.

Jilu Li, John Paden, Carl Leuschen, Fernando Rodriguez-Morales, Richard Hale, Emily Arnold, Reid Crowe, Daniel Gomez-Garcia and Prasad Gogineni, “High-Altitude Radar Measurements of Ice Thickness over the Antarctic and Greenland Ice Sheets as a part of Operation Ice Bridge,” submitted to IEEE Transactions on Geoscience and Remote Sensing, Sept 2011.

Paden, John, Christopher Allen, Sivaprasad Gogineni, Kenneth Jezek, Dorthe Dahl-Jensen, and Lars Larsen, “Wideband measurements of ice sheet attenuation and basal scattering“, *IEEE Geoscience and Remote Sensing Letters*, vol. 2, no. 2, April 2005.

Paden, J., "Synthetic Aperture Radar for Imaging the Basal Conditions of the Polar Ice Sheets", Department of Electrical Engineering and Computer Science, PhD Dissertation, University of Kansas, 08/2006.

Paden, J., T. Akins, D. Dunson, C. Allen, and P. Gogineni, "Ice-sheet bed 3-D tomography", Journal of Glaciology, vol. 56, no. 195, pp. 3-11, 01/2010.

Player, K., Lei Shi, Chris Allen, Carl Leuschen, John Ledford, Fernando Rodriguez-Morales, William Blake, Ben Panzer, and Sarah Seguin, *A Multi-Channel Depth-Sounding Radar with an Improved Power Amplifier*, High-Frequency Electronics, October 2010, p 18-29.

Rodriguez-Morales, F., P. Gogineni, C. Leuschen, C. T. Allen, C. Lewis, A. Patel, L. Shi, W. Blake, B. Panzer, K. Byers, R. Crowe, L. Smith, and C. Gifford, *Development of a Multi-Frequency Airborne Radar Instrumentation Package for Ice Sheet Mapping and Imaging*, Proc. 2010 IEEE Int. Microwave Symp., Anaheim, CA, May 2010, pp. 157 – 160.

F. Rodriguez-Morales, S. Gogineni, C. Leuschen, John Paden, J. Li, C. Lewis, B. Panzer, D. Gomez-Garcia, A. Patel, K. Byers, R. Crowe, K. Player, R. Hale, E. Arnold, L. Smith, C. Gifford, D. Braaten, and C. Panton, Advanced Multi-Frequency Radar Instrumentation for Polar Research, IEEE T. Geoscience and Remote Sensing, vol. 52, no. 5, May 2014, pp. 2824-2842.

Shi, Lei; Allen, C.T.; Ledford, J.R.; Rodriguez-Morales, F.; Blake, W.A.; Panzer, B.G.; Prokopiack, S.C.; Leuschen, C.J.; Gogineni, S.; , "Multichannel Coherent Radar Depth Sounder for NASA Operation Ice Bridge," *Geoscience and Remote Sensing Symposium (IGARSS), 2010 IEEE International* , vol., no., pp.1729-1732, 25-30 July 2010
doi: 10.1109/IGARSS.2010.5649518

Zongbo Wang, Sivaprasad Gogineni, Fernando Rodriguez-Morales, Jie-Bang Yan, John Paden, Carleton Leuschen, Rick Hale, Jilu Li, Calen Carabajal, Daniel Gomez-Garcia, Bryan Townley; Robby Willer; Leigh Stearns; Sarah Child; and David Braaten, Multichannel Wide-band Synthetic Aperture Radar for Ice Sheet Remote Sensing: Development and the First Deployment in Antarctica, accepted for publication IEEE JSTARS in Jan 2015.

Contacts:

Please send all questions and comments to:
cresis_data@cresis.ku.edu